ROAST PROJECT – SIO 217A

Felipe Mejia, Homa Naeimi, Handa Yang, Xiaohui Zhong

1. Introduction

In a normal atmosphere, a large fraction of incoming solar energy is absorbed by the ground and is converted to heat. As a result, the temperature of the atmospheric surface layer rises. The warm air then rises, expands and cools. In general, within the troposphere, temperature decreases as height increases. This relation is described by temperature lapse rate which is defined as (Curry & Webster, 1999):

$$\Gamma = -\frac{dT}{dz}$$

A temperature inversion occurs when there is deviation from this pattern and the normal vertical temperature gradient is inverted (Curry & Webster, 1999). During inversion, a warm, less dense layer of air covers a denser cold layer underneath and creates atmospheric stability. Temperature inversions can be categorized into four different types: ground, marine, subsidence, and frontal (NOAA).

Several meteorological conditions may cause temperature inversion. For example, during the night, the ground acts as a heat sink. The surface layer of the atmosphere loses heat to the ground while above layers retain the heat they absorbed from the ground during the day (Salby, 2012). As a result, a cold layer of air develops underneath a warmer layer, which forms ground inversion. Another scenario is often observed on coastal areas, where cold water acts as a heat sink and decreases air temperature at lower layers, while above layers maintain a higher temperature forming the marine inversion layer. One such situation often occurs in southern California because of the cool ocean water, as well as the warm inland temperatures (Antoine Badan-Dangon, 1991).

Temperature inversion is followed by various consequences, such as freezing rain. When there is a shallow inversion in the presence of snow aloft, the snow melts as it moves through the warm inversion layer and is later super-cooled as it passes through near the surface cold air masses. The super-cooled drops then become ice when they land on the ground and other surfaces (Jones, 1998). Sometimes intense thunderstorms are created due to the intense energy that is released after an inversion layer is broken and normal convection patterns reform (Schaefer, 1986).

Temperature inversion plays a significant role in trapping pollution over megacities by blocking atmospheric flows and causing the atmosphere to become stable. When pollutants from vehicles and industry are emitted into the air, the inversion traps the particles and pollutants near the ground. As a result, smog, which is a gray haze of dust, auto exhaust, and industrial manufacturing, covers the cities, leading to poor air quality (Edinger, 1973). Because temperature inversion has such significant effects on air quality, it is important to better understand this phenomenon, its causes, and consequences.

In this study, a simplified atmospheric model based on the air parcel model described in Pruppacher & Klett (1996) is used to study the effects of temperature inversion on atmospheric convection. Three modeling cases were analyzed. The first case involved a control run without modifying model parameters beyond their default values. The following two cases involved the addition of a temperature inversion at 1.00 km and 0.25 km, respectively. The results from the last two cases were compared against the control run in order to infer variations in atmospheric behaviors in the presence of different temperature inversions.

2. Model description

For the purposes of our model, an "air parcel" is defined as an infinitesimal, well-defined body of air that does not readily mix with the surrounding air, and its temperature is assumed to be generally uniform (Spellman, 2012). To initialize the model, a parcel of air is given an initial temperature and humidity, and its ascent in the atmosphere is described by solving the buoyancy (Eqn. 1) and energy conservation (Eqn. 2) equations:

Equation 1- Buoyancy Force

$$F_{buoyancy} = g(\frac{T_{parcel} - T_{ambient}}{T_{ambient}} - w_l)$$

Equation 2 - Energy Conservation Equation

$$\left(c_p + L_{lv}\frac{dw_s}{dT}\right)dT = -gWdt$$

The following assumptions are made in order to simplify the model: (1) there is no drag force on the parcel due to turbulence along its edges, (2) the ambient temperature profile prior to the temperature inversion (which is described by a dry adiabatic lapse rate and is capped at the surface temperature) is described by the US standard atmosphere, with a surface temperature of 288 K at sea level and a lapse rate of 6.5 K/km, (3) the ambient humidity profile is 80% relative humidity throughout, (4) the parcel's ascent is an adiabatic process, (5) the parcel does not mix, (6) the parcel does not disturb the environment, and (7) the parcel is in mechanical equilibrium with the environment (pressure in the parcel is equal to the ambient pressure).

Although this air parcel model is useful for demonstrating concepts, the simplifications made introduce a degree of inaccuracy. Since the entrainment of ambient air is neglected, the air parcel is assumed to be a closed system, which may lead to higher parcel liquid water content (failed to account for the drying effects of entraining relatively dry ambient air). Additionally, the assumption that the parcel ascension is adiabatic may cause the modeled parcel height to be much higher than actual observations show (Pruppacher & Klett, 1996). The simplified air parcel model also does not account for heating due to incoming short and long wave radiation, or cooling due to radiative losses to the environment.

3. Results & Discussion

From the three cases, it was observed that the temperature inversion limited the parcel height. In the first modeled atmosphere, without a temperature inversion, the parcel's temperature is decreasing. Close to the surface it begins by following the dry adiabatic lapse rate. This is illustrated in figure 1. The parcel begins rising until it reaches about 0.25 km, at which point it reaches its lifting condensation level (LCL) as seen in figure 2. This is the point at which the parcel is fully saturated and follows the wet adiabat. Because the parcel is warmer than the ambient temperature, it continues to rise due to its buoyancy force. It continues rising until it reaches the mixing height, which is the point at which the parcel temperature intersects the ambient temperature and only goes slightly higher due to momentum. This maximum height was observed to be about 1.40 km.

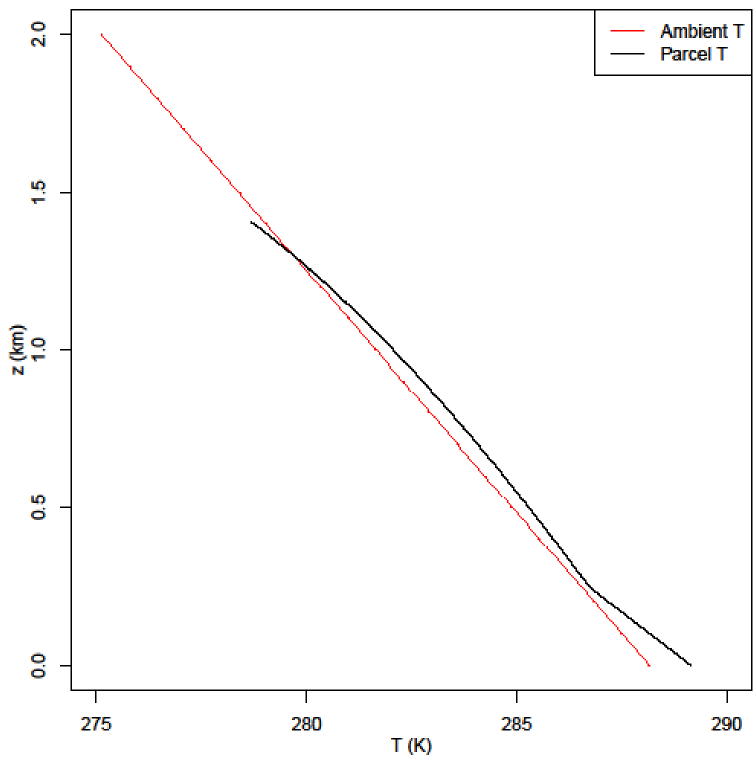

Fig. 1 Parcel height versus parcel temperature (in black) and ambient height versus temperature (in red) for an atmosphere without a temperature inversion.

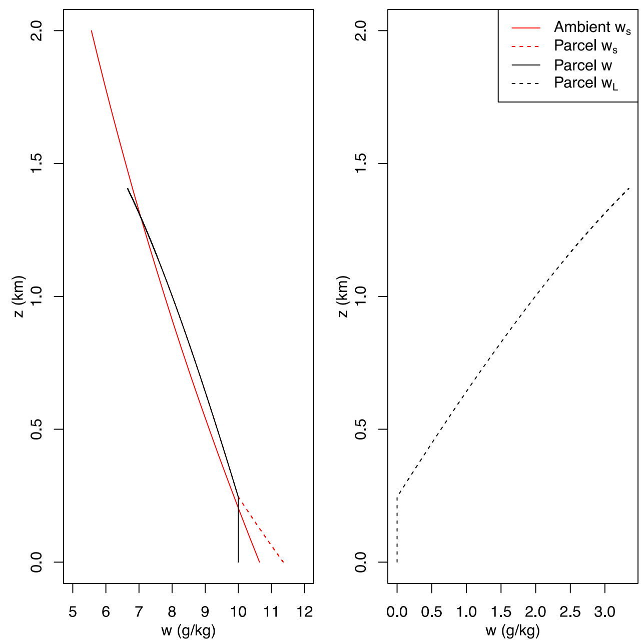

Fig. 2 Height versus ambient saturation pressure, parcel saturation pressure and parcel mixing ratio.

The addition of a temperature inversion to the model caused the parcel to stop rising much closer to the surface than without the temperature inversion. With an inversion at 1.00 km, the parcel reached a maximum height around 1.25 km as shown in figure 3. The parcel stops accelerating soon after reaching its mixing height.

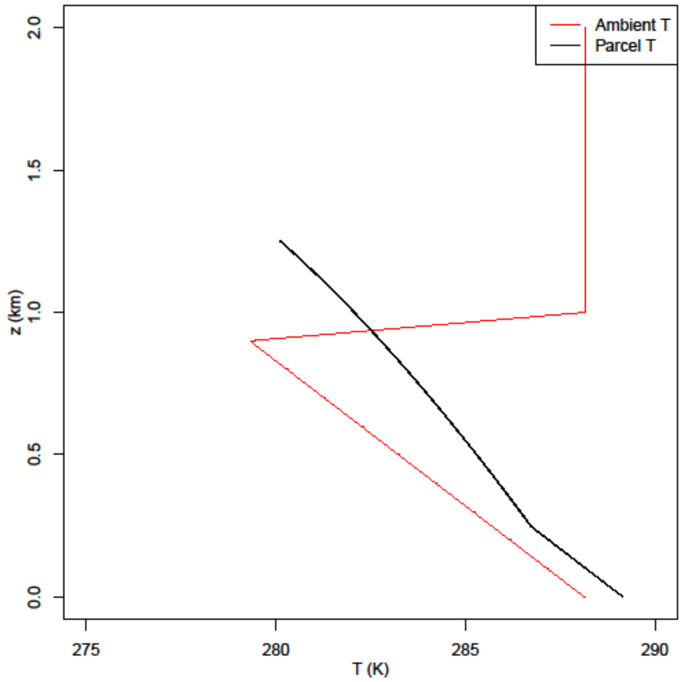

Fig. 3 Parcel height versus parcel temperature (in black) and ambient height versus temperature (in red) for an atmosphere with a temperature inversion at a height of 1 km.

The temperature inversion at 0.25 km limited the parcel height even further. In this atmosphere, the parcel height does not go beyond 0.40 km, as seen in figure 4. As in the previous two cases, the parcel quickly stops accelerating after it reaches the mixing height, suggesting that the point where the parcel reaches the mixing height controls the maximum parcel height.

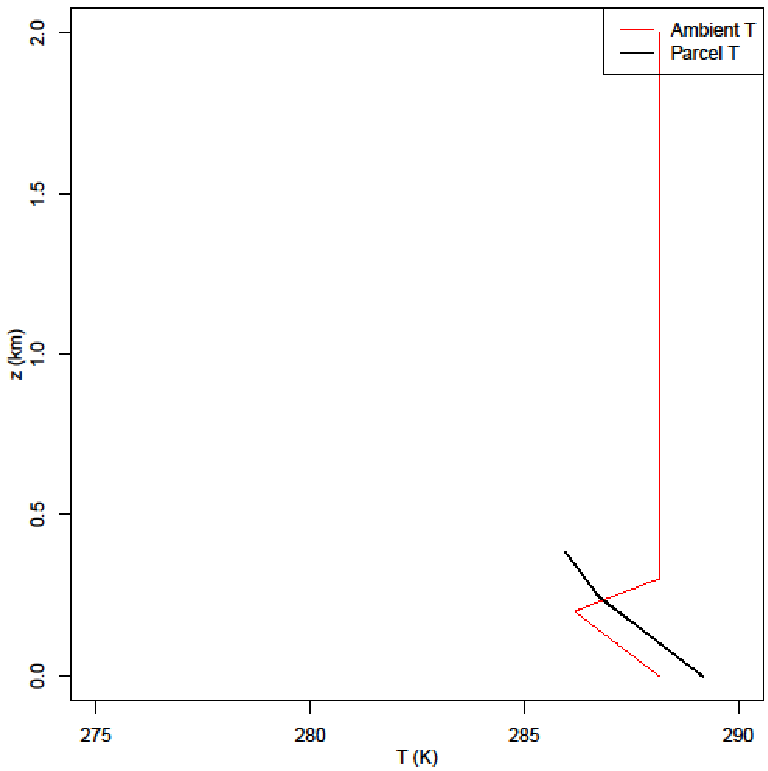

Fig. 4 Parcel height versus parcel temperature (in black) and ambient height versus temperature (in red) for an atmosphere with a temperature inversion at a height of 250 m.

In the three graphs, as the parcel increases in height, its temperature decreases. Close to the surface, the three cases began by following the dry adiabat until they reached the LCL. After the LCL, the three cases began to deviate from each other. Without a temperature inversion, the difference in lapse rate between the parcel and the ambient lapse rate is very small throughout the parcel's ascent, so the parcel continues rising to very high altitudes. With a temperature inversion added, the parcel begins to lose its buoyancy force as it reaches the temperature inversion and decelerates until It can no longer continue rising. This is because, after the temperature inversion, ambient temperature rises which quickly leads to the ambient temperature to be higher than that of the parcel. Once the parcel is cooler than ambient temperature it no longer has the buoyancy force to continue rising so it only rises slightly more due to its momentum. The mixing ratio was found to be unaffected by the addition of the inversion, suggesting that the inversion only affects the parcel's height. Table 1 demonstrates variations in the mixing height of the three different cases.

Table 1 Parcel mixing and maximum heights for the three different cases

	No Temperature Inversion	Temperature inversion at 1.00 km	Temperature inversion at 0.25 km
Parcel Mixing Height	1.25 km	0.90 km	0.30 km
Parcel Maximum Height	1.40 km	1.25 km	0.40 km

As seen in the three modeled atmospheres, the inversion limits atmospheric mixing. The warm inversion layer acts as a lid, making it difficult for the cold air below the inversion to rise. In an atmosphere, such as the one in the control case, pollutants are able to disperse up to 1.40 km, making it more difficult for high concentrations of pollution to accumulate. In this atmosphere, pollution can spread over a larger portion of the atmosphere, so more pollution is needed to reach high concentrations. In addition to this, more of the pollution is located at higher altitudes, so the surface air quality is improved. Similarly, for fog to develop, more water must evaporate to be able to saturate the larger portion of the atmosphere. The fog that does develop in this atmosphere is also located at higher altitudes. With the addition of temperature inversions, the parcel height is capped at 1.25 km and 0.40 km, respectively. This greatly reduces the amount of pollutants needed to create smog. This is the case in Los Angeles where a temperature inversion, like the case with an inversion at 1.00 km, keeps pollution closer to the surface, thus decreasing air quality. Higher concentrations of pollution are reached because the pollution is trapped by the temperature inversion. In San Diego, a temperature inversion, like the one modeled with an inversion at 1.00 km, sometimes develops and leads to dense fog close to the surface. This fog develops because less water is needed to saturate the capped atmosphere. From comparing the two cases with temperature inversions, it is possible to see that the lower the inversion the lower the amount of atmospheric mixing. This reduction in mixing means that the lower the temperature inversion the higher the likelihood of fog or smog to develop.

4. Conclusion

A parcel model was developed and run for three different cases of atmospheric temperature inversions. The three cases were for an atmosphere without a temperature inversion, with one at 1.00 km and with one at 0.25 km. The three cases were picked to compare the effects of a temperature inversion, and they demonstrated how the warm inversion layer reduced the buoyancy force acting on the parcel. The warm inversion layer was found to cap the maximum height of the parcel and reduce atmospheric mixing. This in turn leads to environmental effects such as freezing rain, fog and smog.

Appendix A – Nomenclature

F – Force [N]
g – Gravity of Earth [9.81 m s^{-2}]
T – Temperature [K]
w_l – Liquid water mixing ratio [kg_{H2O} $kg^{-1}{}_{dry\ air}$]
w_s – Saturation mixing ratio [kg_{H2O} $kg^{-1}{}_{dry\ air}$]
c_p – Specific heat capacity at constant pressure [J kg^{-1} K^{-1}]
L_{lv} – Latent heat of vaporization of water [2.27 x 10^6 J kg^{-1}]
W – Vertical velocity of air parcel (dz/dt) [m s^{-1}]

Works Cited

Badan-Dangon, A., Dorman, C. E., Merrifield, M. A., & Winant, C. D. (1991). The lower atmosphere over the Gulf of California. *JOURNAL OF GEOPHYSICAL RESEARCH* , 16,877–16,896.

Curry, J. A., & Webster, P. J. (1999). *Thermodynamics of Atmospheres & Oceans.* ACADEMIC PRESS.

Edinger, J. G. (1973). Vertical distribution of photochemical smog in Los Angeles basin. *Environmental Science and technology* , 242-252.

Jones, K. F. (1998). A simple model for freezingrain ice loads. *Atmospheric Research* , 87-97.

NOAA. (n.d.). Retrieved 11 14, 2012, from http://www.wrh.noaa.gov/slc/climate/TemperatureInversions.php

Pruppacher, H. R., & Klett, J. D. (1996). Microphysics of Clouds and Precipitation. Dordrecht: Kluwer Academic Publishers.

Salby, M. L. (2012). *Physics of the atmosphere and climate .* New York: Cambridge University Press.

Schaefer, J. T. (1986). Severe Thunderstorm Forecasting: A Historical Perspective. *Weather and Forcasting* , 164-189.

Spellman, F. R. (2012). Environmental Impacts of Hydraulic Fracturing. Boca Raton: Taylor & Francis Group.